

Molecular dynamics simulation on the tribology properties of two hard nanoparticles (diamond and silicon dioxide) confined by two iron blocks

Chengzhi Hu^a, Minli Bai^a, Jizu Lv^{a,*}, Zhihai Kou^b, Xiaojie Li^c

^a School of Energy and Power Engineering, Dalian University of Technology, Dalian 116024, China

^b Faculty of Aerospace Engineering, Shenyang Aerospace University, Shenyang 110136, China

^c The State Key Laboratory of Structural Analysis for Industrial Equipment, Dalian University of Technology, Dalian 116024, China



ARTICLE INFO

Article history:

Received 30 December 2014

Received in revised form

15 April 2015

Accepted 27 April 2015

Available online 14 May 2015

Keywords:

Diamond nanoparticle

Silicon dioxide nanoparticle

Molecular dynamics

Tribology behaviors

ABSTRACT

The tribology behaviors of diamond and silicon dioxide (SiO_2) nanoparticles were examined via molecular dynamics simulations; four cases were simulated. At low velocity and low load, the nanoparticles separated the two blocks from each other and acted as ball-bearings. The plastic deformation, temperature distribution, and friction force were all improved due to the action of the nanoparticles. However, the crushing of the SiO_2 nanoparticles was accompanied by deformation-induced loss of the rolling effect, when the load was increased. Without nanoparticles, a transfer layer formed at high velocity and low load. The two nanoparticles provided support for a certain duration. However, at high velocity and high load, the support effect of these nanoparticles was lost in a short sliding time.

© 2015 Elsevier Ltd. All rights reserved.

1. Introduction

The addition of nanoparticles with sizes of 1–120 nm to lubricants as anti-friction and anti-wear additives has received significant attention in recent years [1–3]. Experimental results show that various nanoparticles such as metal [2,4–8], metal oxides [9–14], sulfides [15–20], non-metals [21–25] and rare earths [26] can improve the friction reduction and anti-wear behaviors of the lubricants. However, the lubrication mechanisms of these nanoparticles are still not completely understood [27].

These lubrication mechanisms are currently investigated primarily by experimental methods. In fact, researchers have proposed several mechanisms, based on the analysis of scanning electron microscopy images and energy dispersive spectrometry spectrum of the wear surface. These mechanisms include (a) rolling friction [21,22,28,29], (b) third-body material [11,30], (c) surface protective film [9,11,31], and (d) a self-repair effect [2,18]. However, these mechanisms are speculative, i.e., based on experimental results only, and lack theoretical support and direct evidences. The lubrication state in an experiment represents, in general, a combination of boundary lubrication, thin film lubrication, and elastohydrodynamic lubrication. Moreover, the lubrication mechanisms of nanoparticles vary with the lubrication states. There is also no consensus regarding the dominant

mechanisms, which lead to friction reduction and anti-wear of nanolubricated surfaces. For example, Ghaednia and Jackson [27] were uncertain as to whether nanoparticles, which can roll and act as nano ball-bearings, are likely to induce abrasive wear, or form tribolayers on the asperity tops. Chou and Lee [23] questioned whether nano-diamond particles truly acted as ball bearings. These issues are not easily resolved experimentally and therefore, additional research methods are essential to their resolution.

The molecular dynamics (MD) simulation method is generally considered a very useful complementary tool to experimental studies on nanotribological behaviors [3]. Many studies have reported detailed friction processes at the atomic level, which were obtained by using the MD method [32–37]. Several MD simulations of the friction reduction and anti-wear mechanisms of nanoparticles have been conducted. For example, Lv et al. [38] studied the friction behaviors of Cu–argon nanofluids between two solid plates by analyzing the movement of nanoparticles under different pressures. However, the mechanical properties of the friction system were not investigated. In previous work [32], we simulated the effect of nanoparticles on the rheological properties of a lubricant film. The effect of nanoparticles on the mechanical properties of the friction pair was, however, not considered. Very recently, we studied the effect of soft nanoparticles (copper) on the solid contact between friction surfaces [39]. The results revealed that, at low velocity, a Cu nano-film formed on the friction surface provided excellent lubrication. Although helpful, these studies do not elucidate the lubrication mechanisms of nanoparticles. The lubrication mechanisms will vary

* Corresponding author. Tel.: +86 13942601557; fax: +86 411 84706305.
E-mail address: ljizu@dlut.edu.cn (J. Lv).

with the nanoparticle type. However, studying the tribological properties of all nanoparticles is impractical and a classification into soft and hard particles represents a more efficient manner of performing such investigations. As such, in this work, we investigate the friction processes of hard particles via MD simulations.

Diamond and silicon dioxide (SiO_2) are two typical hard nanoparticles and many experimental studies have reported improvements in the friction properties, due to their addition [21, 22, 24, 40–49]. The lubrication mechanisms of these two nanoparticles, which are used as lubricant additives, exhibit similar characteristics namely: (a) they act as billions of rolling particles between the rubbing surfaces [21, 22, 29, 41, 42, 45] and (b) they separate the rubbing faces and prevent direct contact [21, 41, 45, 46]. However, the tribology properties differ somewhat due to differences in the atom species, structure, and hardness of the two nanoparticles. SiO_2 nanoparticles are cheap and readily accessible. We believe that SiO_2 replacement of diamond nanoparticles is feasible only under some lubrication conditions. To address this problem, we will compare the tribological behaviors of the two nanoparticles.

Nanoparticles perform most efficiently under boundary and mixed lubrication conditions [2, 19, 21, 22, 30, 31, 50, 51]. Under mixed and boundary lubrication, there is always solid contact between the friction surfaces, which in turn leads to local surface breakage. The improved lubrication effect of nanoparticles on the rubbing surfaces is essential to the anti-wear and friction reduction properties. Therefore, in this work, the effect of hard nanoparticles (diamond and SiO_2) on the solid contact between friction surfaces, is investigated via MD simulations.

2. Model and simulation details

2.1. Model setup

Snapshots of the simulated systems are shown in Fig. 1. Two similar iron (Fe) blocks acted as the friction pair. When no nanoparticles were present, the two blocks contacted each other directly (Fig. 1a). A nanoparticle with a radius of 15 Å was then placed between the two blocks (Fig. 1b) to prevent their direct contact. This nanoparticle was free to move and no artificial constraint was applied. Periodic boundary conditions were imposed in the x and z directions. As in our previous study, the blocks consisted of six layers, namely: rigid layers (1, 6), thermostat layers (2, 5) and free deformable layers (3, 4). Nose–Hoover thermal baths [52] were attached to the thermostat layer in

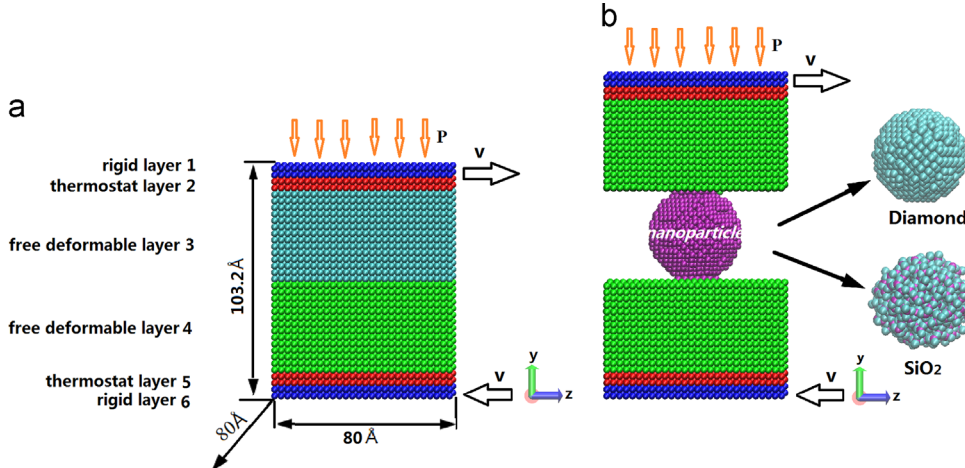


Fig. 1. Snapshot of simulation system without nanoparticle (a) and the system with hard nanoparticle (diamond and SiO_2) (b). Purple and cyan points in the SiO_2 nanoparticle indicate silicon and oxygen atoms, respectively. (For interpretation of the references to color in this figure legend, the reader is referred to the web version of this article.)

order to fix the temperature at 300 K. Furthermore, each rigid layer consisted of stationary atoms, whereas those in the free deformable layers were unconstrained and moved freely due to the interatomic forces. The two rigid layers slid in opposite directions at velocity v . A normal load (P) was imposed on the upper rigid layer, and the lower rigid layer was immobile in the y direction.

2.2. Molecular dynamics

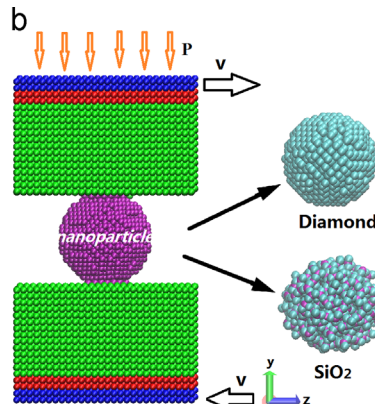
The interactions between Fe atoms were modeled by an embedded atom method (EAM) potential which can describe the properties of metallic systems very well. The EAM potential parameters used in the study were developed by Bonny et al. [53]. A Tersoff potential [54] was adopted for carbon–carbon (C–C) interactions. The BKS potential [55,56] was used to model SiO_2 nanoparticle. The partial charge of 2.4e for silicon atoms and –1.2e for the oxygen atoms were used in the BKS potential to provide electrostatic interactions. The values of the BKS potential parameters for SiO_2 can be found in the work [56]. The interactions between Fe–C, Fe–Si, and Fe–O were modeled by 12–6 Lennard Jones potential and the potential parameters are given in Table 1.

2.3. Simulation procedure

The simulations were all performed using the classical open source MD LAMMPS code [60]. Three steps were taken to realize the simulation. First, the system was relaxed for 200 ps and an equilibrium state was achieved. During this step, the canonical ensemble (NVT) was applied to both the thermostat and free deformable layers, i.e., layers (2, 5) and (3, 4), respectively. The load P was then gradually applied to the upper rigid layer and we equilibrated the systems again. During this re-equilibration, the

Table 1
Lennard Jones energies (ϵ) and distances (σ) for Fe, Si, O, and C [57–59].

Species	ϵ (eV)	σ (Å)
Fe–Fe	0.527	2.321
Si–Si	0.0175	3.826
O–O	0.00738	2.96
Fe–C	0.02495	3.7
Fe–Si	0.096	3.0735
Fe–O	0.06237	2.6405



NVT ensemble used for the free deformable layers, was converted to the micro-canonical ensemble (NVE). The upper and lower rigid layers were then pulled in opposite directions at velocity v . The sliding friction was performed for 1600 ps. In this study, we used the velocity Verlet algorithm [61] to calculate the atomic motions; a time step of 0.002 ps was used for the simulations. During the sliding simulation, the evolution of friction was tracked by monitoring the tangential z-direction forces required to maintain the constant velocity of the rigid layers.

3. Results and discussion

In our previous work [39], we found that the mechanisms of nanoparticles leading to improved friction properties vary with the sliding velocity. In this study, the tribological properties of diamond and SiO_2 nanoparticle will also be analyzed based on low and high velocity.

3.1. Friction state with low velocity

A sliding velocity of 10 m/s was considered.

3.1.1. Friction process under a low load

Fig. 2 shows the friction states, which occur under a low load of 500 MPa. Selected atoms (blue and red atoms) in the two blocks

have been colored differently to show the plastic deformation and interfacial slip during sliding. In the absence of nanoparticles, the two blocks were joined by applying a normal load. The straight markers became bent due to the shear stress, and features typical of deformation microstructures formed in both blocks. The two blocks were separated from each other when hard nanoparticles (diamond and SiO_2) were added. This is consistent with findings of Tao et al. [21], Peng et al. [41,45], and Mochalin et al. [46] who proposed that the two nanoparticles separate the rubbing faces and thereby prevent their direct contact. The markers remained straight during the sliding friction process, indicating that the friction pairs were only slightly deformed. Direct contact between the friction surfaces and plastic deformation in the friction pairs should result in adhesive fatigue and contact fatigue. Therefore, the friction behaviors of the hard nanoparticles (**Fig. 2**) should reduce the wear rate and improve the morphology of the worn surface. In fact, the experimental results indicate that, as lubricating oil additives, the two nanoparticles both reduce wear and smooth the worn surfaces more than the pure base oil [21,24,41]. Analyzing the displacement of the marker (yellow atoms) in the nanoparticles reveals that both nanoparticles acted as ball-bearings between the friction surfaces. In addition, plotting the angular velocity around the x-axis (**Fig. 3**) shows that the nanoparticles rotated clockwise for most of the sliding process. This provides direct evidence for the mechanism of anti-wear and friction reduction by nanoparticles; i.e., spherical nanoparticles are

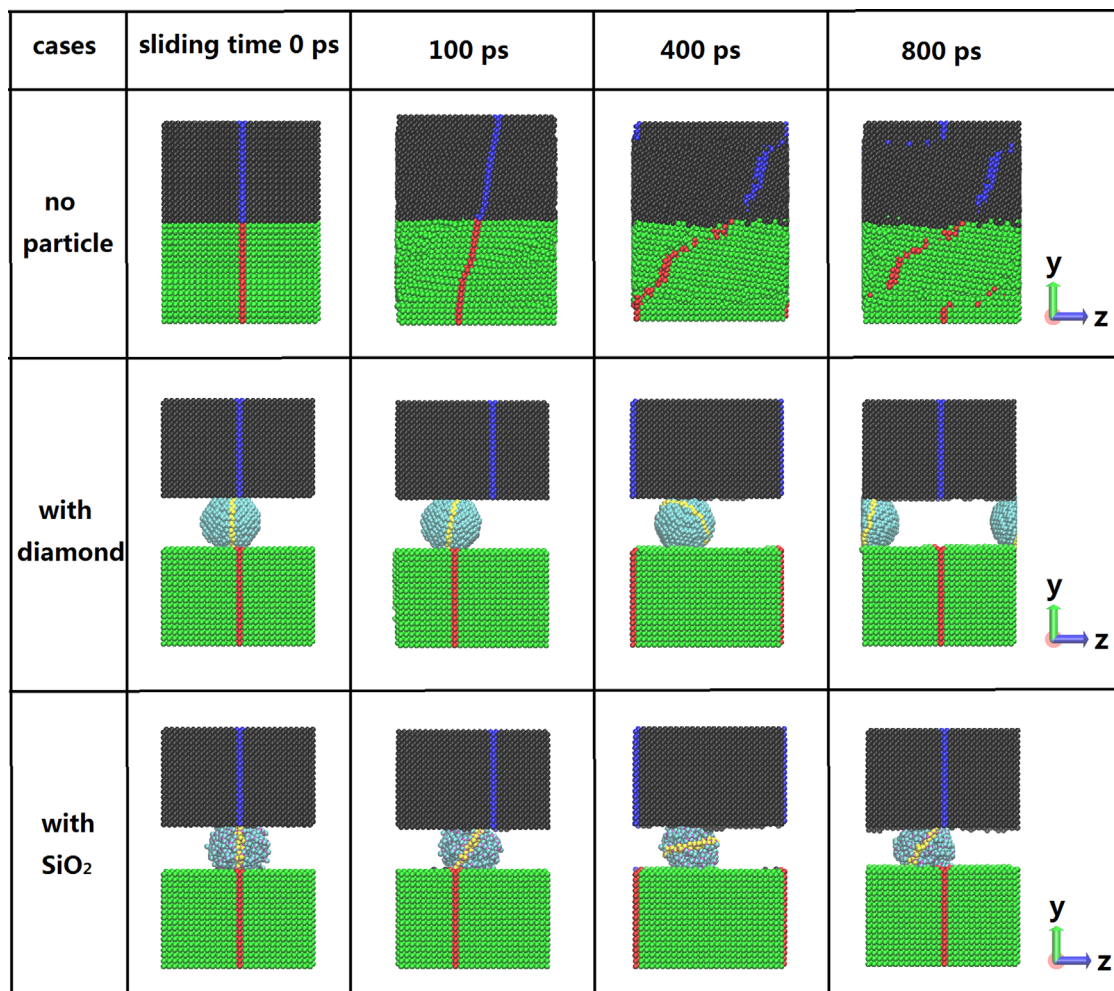


Fig. 2. Still images of friction state at different sliding times. The blue and red atoms are the markers used to visualize the deformation. In order to make figures clear, the two blocks are colored differently. Part atoms on the two nanoparticles are color-coded yellow to act as markers to show the rotation of nanoparticles. $v=10 \text{ m/s}$, $P=500 \text{ MPa}$. (For interpretation of the references to color in this figure legend, the reader is referred to the web version of this article.)

likely to roll between the rubbing surfaces and convert the sliding friction into the mixed friction of sliding and rolling [21, 22, 29, 41, 42, 45].

Fig. 4 shows the effect of the two nanoparticles on the morphology of the friction surface. Grooves formed with increasing sliding time, proving that the two nanoparticles had cutting action during rolling friction. In the case of boundary lubrication, the solid contact between the friction surfaces result mainly from asperity contacts. These asperities are polished by the hard nanoparticles, which penetrate the contact area. Thus, the cutting action of the two nanoparticles is benefit to the improvement of morphology of rough surface. Tao et al. [21], Peng et al. [45], Chou et al. [47], Ivanov et al. [44], and Sia et al. [49] proposed that diamond and SiO_2 will also exert a polishing action on the rubbing surfaces. In fact, profiles measured across the test material and the rubbing surface after friction tests [21, 45, 49] revealed that the rubbing surfaces lubricated by diamond and SiO_2 nanoparticles

were smoother than those of the test materials. Therefore, under boundary lubricating conditions, the two hard nanoparticles have a polishing effect on the friction surfaces.

The temperature distributions of the solid contact surfaces have a significant effect on the tribological characteristics. This was demonstrated by dividing the system into several layers along the y -axis, determining the temperature profile, and computing the average temperature of each layer. Fig. 5 shows the temperature distributions along the y -dimension, at a sliding time of 400 ps. Since the direct contact of friction pairs is prevented, the system containing the two hard nanoparticles exhibits lower temperatures compared to its no-nanoparticle counterpart. Without nanoparticles, the temperature of the free deformable layers increased significantly due to severe shear deformation. This suggests that hard-nanoparticle-added lubricants were effective in reducing the temperature of the friction pair. This finding concurs with previous experimental studies. Ivanov et al. [44]

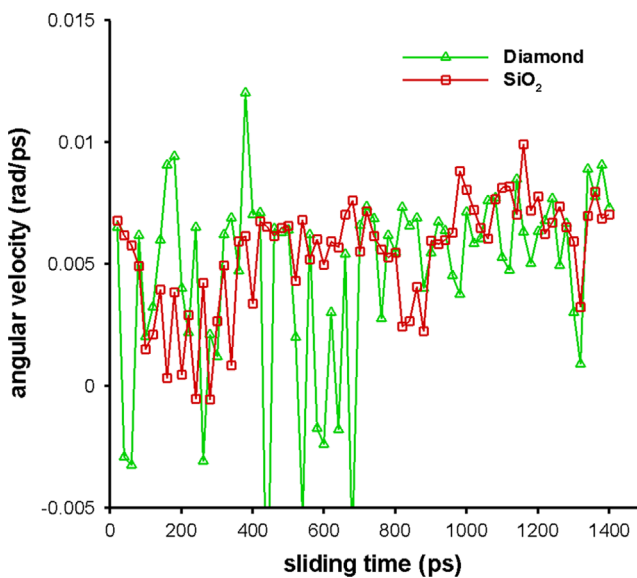


Fig. 3. Angular velocities of diamond and SiO_2 nanoparticles around x -axis. A positive value suggests the clockwise rotation. $v=10 \text{ m/s}$, $P=500 \text{ MPa}$.

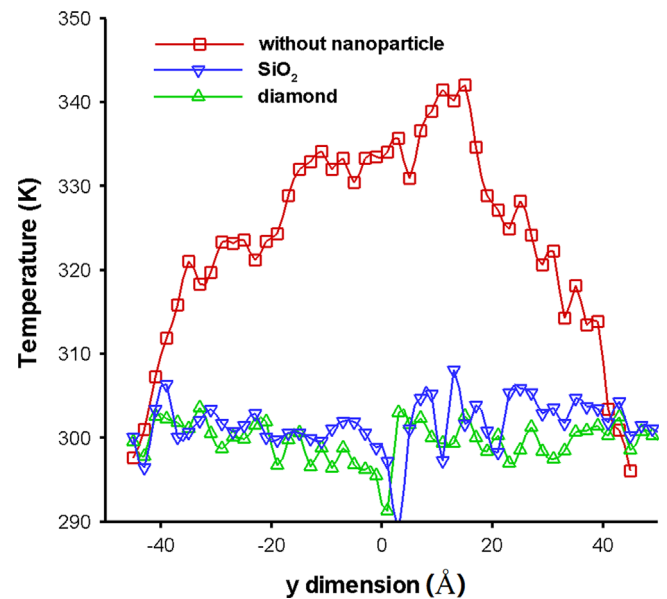


Fig. 5. Temperature profiles along y dimension at a sliding time of 400 ps. $v=10 \text{ m/s}$, $P=500 \text{ MPa}$.

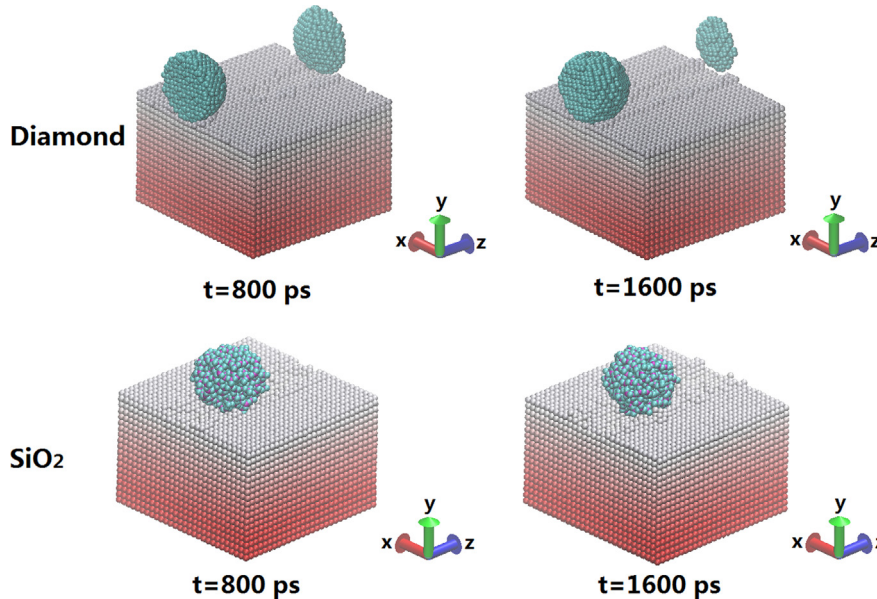


Fig. 4. Morphology changes of friction surface of lower block. The lower block is color coded according to the position on the y -axis. $v=10 \text{ m/s}$, $P=500 \text{ MPa}$.

monitored the temperature at the friction pair and found that, compared to base oil, a 100° lower temperature of the friction surfaces was obtained when nanodiamond was used as the lubricant additive. Furthermore, Liu et al. [48] found that ultra-dispersed diamond led to a reduction in the bulk temperature of the friction surface.

3.1.2. Friction process under a high load

Fig. 6 compares the friction states of diamond and SiO_2 nanoparticles under a high load of 1000 MPa. To facilitate the observation, the upper block is not shown in the figure. As in the case of low load, the two nanoparticles separated the blocks and the friction pairs exhibited only a small amount of plastic deformation. In addition, owing to its high hardness, the shape of the diamond nanoparticle remained unchanged under high loading. The SiO_2 nanoparticle, in contrast, was crushed under the high pressure. The displacement of the markers (yellow atoms) on the nanoparticles confirmed that the diamond nanoparticle still acted as a ball-bearing between the friction surfaces. However, deformation-induced loss of the rolling effect occurred in the case of the SiO_2 nanoparticle. A plot of the angular velocities around the x -axis, under this high load, (**Fig. 7**) shows that the SiO_2 nanoparticle has almost no average angular velocity. Therefore, under high load, the friction state of the SiO_2 nanoparticle is constituted solely of sliding friction; this differs from the frictional state under the low load condition. Furthermore, the SiO_2 nanoparticle was pressed into, and moved with, the lower block and hence, there was no groove on the friction surface (**Fig. 6**).

3.1.3. Friction force

The friction force is plotted in **Fig. 8**. In our previous study [39], we found that without nanoparticles a 500 MPa load resulted in a friction force of ~ 5 GPa. As **Fig. 8** shows, the friction force was significantly reduced with the addition of diamond and SiO_2 nanoparticles. The friction force of diamond was, however, smaller than that of SiO_2 under both low and high loads. This difference results from the smaller interaction strength of Fe-C compared to those of Fe-Si and Fe-O (**Table 1**). Furthermore, owing to the deformation behavior, the contact area between the SiO_2 and the blocks was larger than that of the diamond nanoparticle. Under the high load condition, the diamond converted the sliding friction

to rolling friction, whereas the friction state of SiO_2 was described solely by sliding friction.

The increased temperature of the friction pair is attributed to the friction power, which is expressed as a function of the friction force and the sliding velocity. Therefore, diamond addition resulted in a lower temperature of the iron blocks compared to that resulting from adding SiO_2 , as shown in **Fig. 5**.

3.2. Friction state with high velocity

A sliding velocity of 500 m/s was also considered. This velocity is higher than that at which the transition to velocity weakening of the friction force [37,62,63] in sliding contact, occurs.

3.2.1. Friction process under a low load

We show in **Fig. 9** and **Fig. 10** the friction processes of diamond and SiO_2 nanoparticles under a low load of 500 MPa. The markers (yellow atoms) in nanoparticles, reveal the rolling effect of both nanoparticles. Without nanoparticles, a strongly modified material

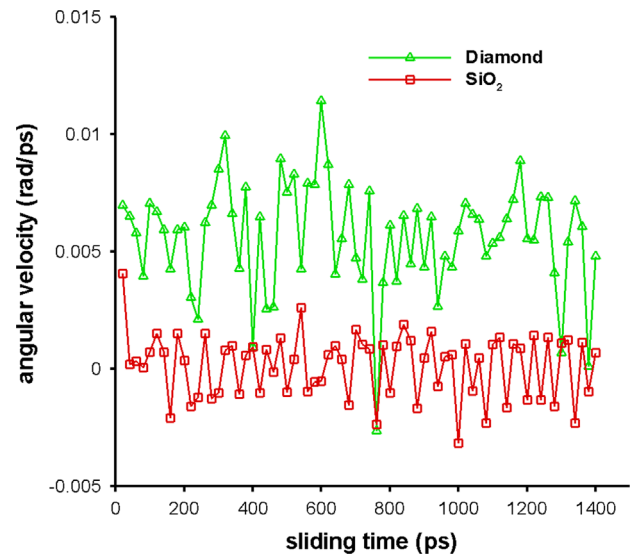


Fig. 7. Angular velocities of diamond and SiO_2 nanoparticles around x -axis. $v=10 \text{ m/s}$, $P=1000 \text{ MPa}$.

cases	t=100 ps	t=800 ps	t=1600 ps	nanoparticle's shape
diamond			unloading state loading state	unloading state loading state
SiO_2			unloading state loading state	unloading state loading state

Fig. 6. Friction states and the shape of nanoparticle under a high load. To facilitate the observation, upper blocks were not shown. The color rule for atoms is the same as that in **Fig. 2**. $v=10 \text{ m/s}$, $P=1000 \text{ MPa}$. (For interpretation of the references to color in this figure legend, the reader is referred to the web version of this article.)

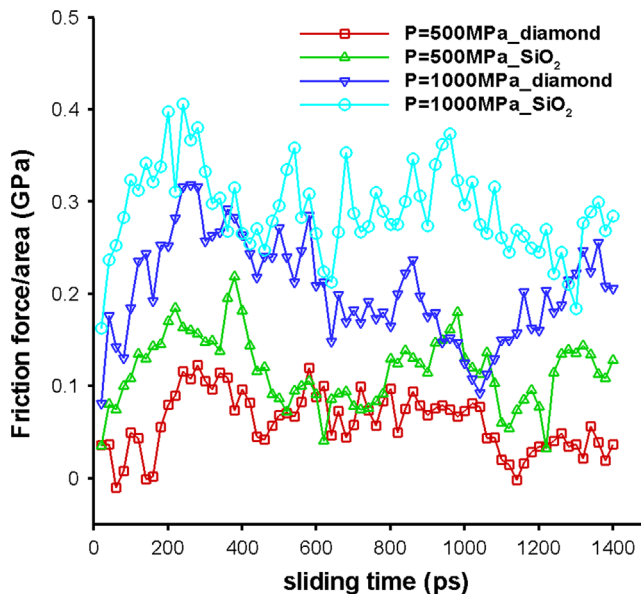


Fig. 8. Friction force with respect to sliding time. The values on the y-axis are divided by the area of block in xz plane. $v=10 \text{ m/s}$.

region (i.e., the transfer layer) formed adjacent to the interface of the two blocks, as shown in Fig. 9. Rigney et al. [37], Hammerberg et al. [62], and Kim et al. [64] also reported the formation of a transfer layer. In our previous work [39], a stable transfer layer also formed when a soft nanoparticle (copper) was added. However, the friction state stemming from the use of the two hard nanoparticles, prevented the direct contact of the blocks at high velocity. When the diamond nanoparticle was added, the formation of the transfer layer was prevented for the entire friction process. Fig. 10 shows that the SiO_2 nanoparticle prevented the direct contact of the two blocks only initially. However, the direct contact of the blocks at sliding times higher than 1100 ps, led to the formation of the transfer layer. This indicates that diamond nanoparticles are more effective than SiO_2 in improving the high-velocity tribological properties. This difference in tribological properties results from differing responses to the load; i.e., the SiO_2 nanoparticle deformed under the load (Fig. 10), whereas the diamond did not. Moreover, the atomic interaction strength of the Fe–Si and Fe–O was higher than that of the Fe–C (Table 1). The SiO_2 nanoparticle led, therefore, to more severe plastic deformation on the friction surfaces and the cutting depth increased faster than in the case of its diamond counterpart. As such, the two blocks came into direct contact at a sliding time of 1100 ps

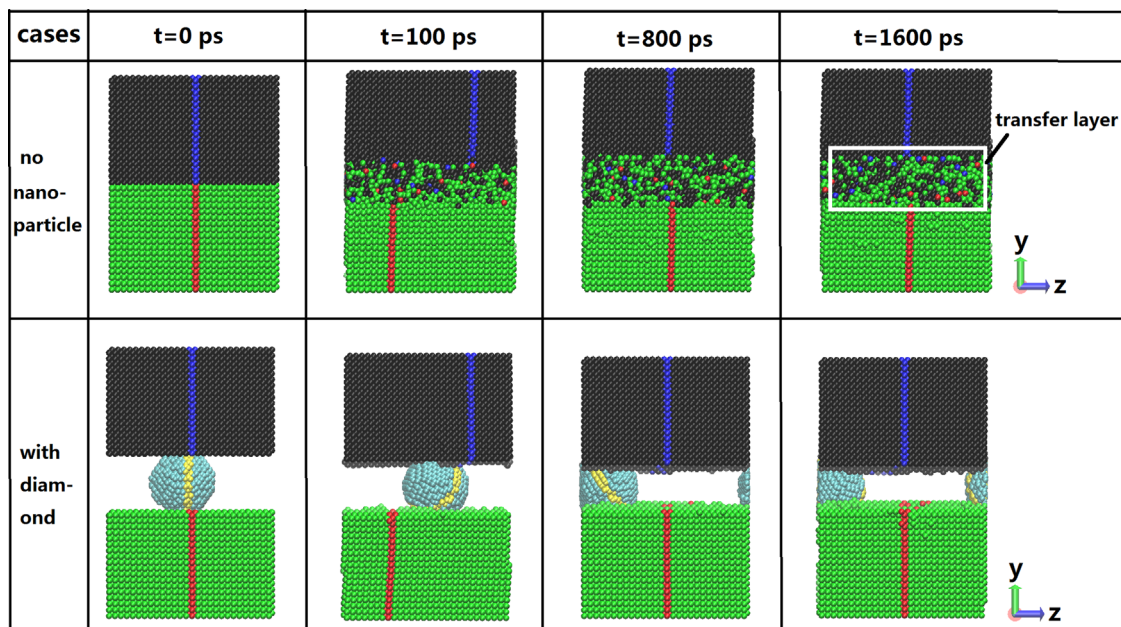


Fig. 9. Friction state at different sliding times. The color rule for atoms is the same as that in Fig. 2. $v=500 \text{ m/s}$, $P=500 \text{ MPa}$. (For interpretation of the references to color in this figure legend, the reader is referred to the web version of this article.)

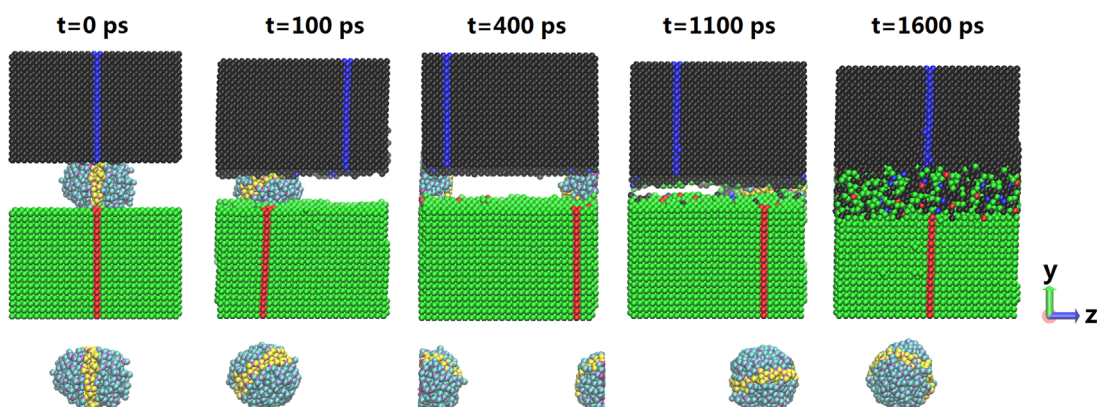


Fig. 10. Friction state of SiO_2 nanoparticle at different sliding times (upper). To observe the motion state of particle, the SiO_2 nanoparticle was displayed separately (lower). The color rule for atoms is the same as that in Fig. 2. $v=500 \text{ m/s}$, $P=500 \text{ MPa}$. (For interpretation of the references to color in this figure legend, the reader is referred to the web version of this article.)

(Fig. 10), which led to the formation of the transfer layer near the interface.

Fig. 11 shows the temperature distributions at a sliding time of 800 ps where both nanoparticles provided excellent support for the blocks. As Lin et al. [63], Kim et al. [64], and Karthikeyan et al. [65] previously reported, there was a sharp spike in the temperature in the middle region (transfer layer) when no nanoparticle was added. The addition of the two nanoparticles led to a significant improvement in the temperature distribution compared with the case without nanoparticles.

3.2.2. Friction process under a high load

The friction states changed significantly with increasing load. Fig. 12 shows the friction processes of the two nanoparticles under a

high load of 1000 MPa. Both nanoparticles were trapped in the transfer layers, which formed after only a short sliding time. The formation of the layers was accelerated (compared to lower loads of e.g., 500 MPa) owing to the rapid increase in the cutting depths of the nanoparticles. Plastic deformation, nanocrystallization, amorphization, frictional heating, and non-equilibrium material flow phenomena are common features of tribological interactions in a transfer layer [37,62,63]. These features have considerable influence on both the friction and wear properties of a sliding system. Furthermore, the tribological properties of the transfer layer may be influenced by the hard nanoparticles trapped therein. This possibility will be examined in future work.

4. Conclusions

In this work, molecular dynamic simulations were used to investigate the frictional properties of two hard nanoparticles (diamond and SiO₂) and reveal the mechanisms governing their anti-wear and friction reduction behavior. The following conclusions can be drawn from this study:

- (1) The tribology behaviors of the two nanoparticles were quite similar under a low load (500 MPa) and a low sliding velocity (10 m/s). The two blocks were separated from each other by the diamond and SiO₂ nanoparticles and the friction pairs were only slightly deformed. This resulted in both improved temperature distributions and friction forces. The nanoparticles acted as ball-bearings and converted the sliding friction into mixed friction consisting of both sliding and rolling. The morphological changes were also analyzed and the results indicated that hard nanoparticles had a polishing effect on the friction surfaces. Moreover, the tribology properties of diamond changed only slightly when the load was increased to 1000 MPa. In contrast, the crushing of the SiO₂ nanoparticle under the load was accompanied by a deformation-induced loss of the rolling effect.
- (2) Without nanoparticles, a transfer layer formed at a high velocity and low load of $v=500$ m/s and $P=500$ MPa,

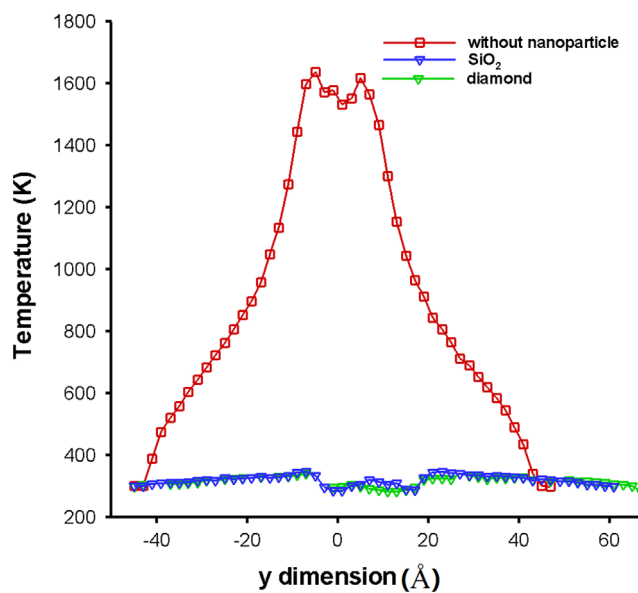


Fig. 11. Temperature profiles along y dimension at a sliding time of 800 ps. $v=500$ m/s, $P=500$ MPa.

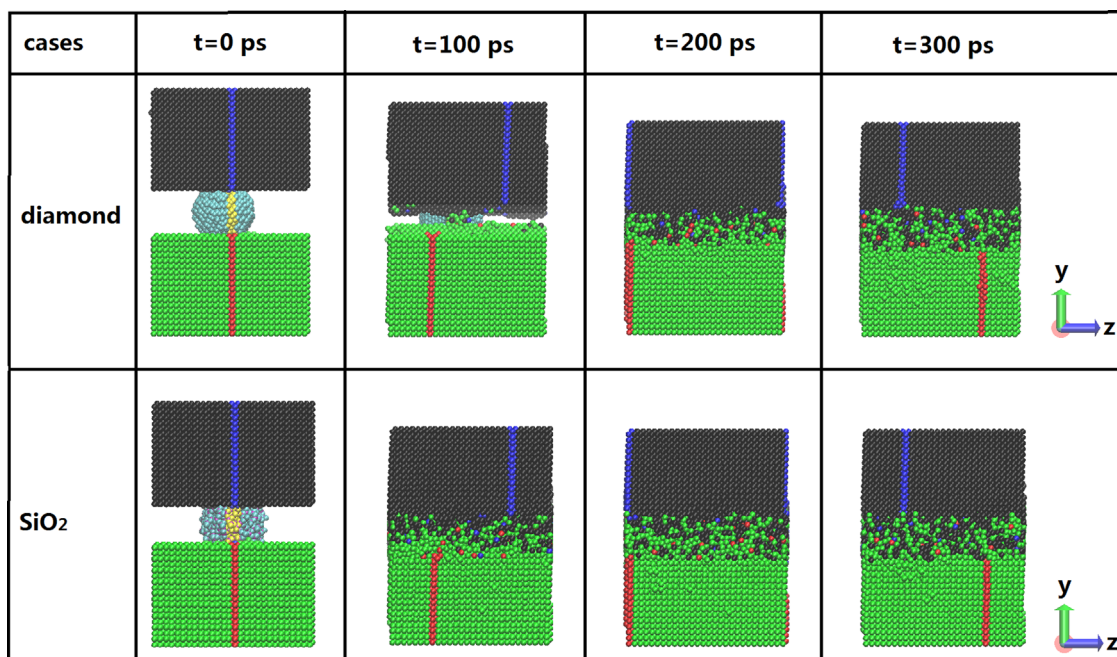


Fig. 12. Friction state at different sliding times. The color rule for atoms is the same as that in Fig. 2. $v=500$ m/s, $P=1000$ MPa. (For interpretation of the references to color in this figure legend, the reader is referred to the web version of this article.)

respectively. However, the diamond nanoparticle prevented direct contact between the two blocks during the entire simulation and no transfer layer was formed. The SiO₂ nanoparticle provided support for only a certain time during the simulation. The temperature distributions of the friction systems were significantly improved owing to the support effect of the two nanoparticles. In addition, the nanoparticles still acted as ball-bearings. However, at high velocity and high load (500 m/s, 1000 MPa), the support effect of the nanoparticles was lost in a short sliding time, and transfer layers were rapidly formed.

Acknowledgments

This work is supported by National Natural Science Foundation of China (Grant nos. 51476019, 51276031, 51376002 and 51206115).

References

- [1] Tang Z, Li S. A review of recent developments of friction modifiers for liquid lubricants (2007–present). *Curr Opin Solid State Mater* 2014;18:119–39.
- [2] Choi Y, Lee C, Hwang Y, Park M, Lee J, Choi C, et al. Tribological behavior of copper nanoparticles as additives in oil. *Curr Appl Phys* 2009;9:124–7.
- [3] Guo D, Xie G, Luo J. Mechanical properties of nanoparticles: basics and applications. *J Phys D: Appl Phys* 2014;47:013001–25.
- [4] Qiu S, Zhou Z, Dong J, Chen G. Preparation of Ni nanoparticles and evaluation of their tribological performance as potential additives in oils. *ASME J Tribol* 2001;123:441–3.
- [5] Kolodziejczyk L, Martínez-Martínez D, Rojas TC, Fernández A, Sánchez-López JC. Surface-modified Pd nanoparticles as a superior additive for lubrication. *J Nanopart Res* 2006;9:639–45.
- [6] Chou R, Battez AH, Cabello JJ, Viesca JL, Osorio A, Sagastume A. Tribological behavior of polyalphaolefins with the addition of nickel nanoparticles. *Tribol Int* 2010;43:2327–32.
- [7] Pan Q, Zhang X. Synthesis and tribological behavior of oil-soluble Cu nanoparticles as additive in SF15W/40 lubricating oil. *Rare Met Mater Eng* 2010;39:1711–4.
- [8] Sánchez López JC, Abad MD, Kolodziejczyk L, Guerrero E, Fernández A. Surface-modified Pd and Au nanoparticles for anti-wear applications. *Tribol Int* 2011;44:720–6.
- [9] Gao Y, Chen G, Oli Y, Zhang Z, Xue Q. Study on tribological properties of oleic acid-modified TiO₂ nanoparticle in water. *Wear* 2002;252:454–8.
- [10] Radice S, Mischler S. Effect of electrochemical and mechanical parameters on the lubrication behaviour of Al₂O₃ nanoparticles in aqueous suspensions. *Wear* 2006;261:1032–41.
- [11] Hernández Battez A, González R, Viesca JL, Fernández JE, Díaz Fernández JM, Cu O Machado A. ZrO₂ and ZnO nanoparticles as antiwear additive in oil lubricants. *Wear* 2008;265:422–8.
- [12] Ma J, Bai M. Effect of ZrO₂ nanoparticles additive on the tribological behavior of multialkylated cyclopentanes. *Tribol Lett* 2009;36:191–8.
- [13] Hernández AB, Viesca JL, González R, Blanco D, Asedegbeaga E, Osorio A. Friction reduction properties of a CuO nanolubricant used as lubricant for a NiCrBSi coating. *Wear* 2010;268:325–8.
- [14] Zhou GH, Zhu Y, Wang X, Xia M, Zhang Y, Ding H. Sliding tribological properties of 0.45% carbon steel lubricated with Fe₃O₄ magnetic nanoparticle additives in base oil. *Wear* 2013;301:753–7.
- [15] Rapoport L, Leshchinsky V, Lapsker I, Volovik Y, Nepomnyashchy O, Lvovsky M, et al. Tribological properties of WS₂ nanoparticles under mixed lubrication. *Wear* 2003;255:785–93.
- [16] Leshchinsky V, Popovitz-Biro R, Gartsman K, Rosentsveig R, Rosenberg Y, Tenne R, et al. Behavior of solid lubricant nanoparticles under compression. *J Mater Sci* 2004;39:4119–29.
- [17] Kang X, Wang B, Zhu L, Zhu H. Synthesis and tribological property study of oleic acid-modified copper sulfide nanoparticles. *Wear* 2007;265:150–4.
- [18] Mosleh M, Atnafu ND, Belk JH, Nobles OM. Modification of sheet metal forming fluids with dispersed nanoparticles for improved lubrication. *Wear* 2009;267:1220–5.
- [19] Kalin M, Kogovsek J, Remškar M. Mechanisms and improvements in the friction and wear behavior using MoS₂ nanotubes as potential oil additives. *Wear* 2012;280:36–45.
- [20] Yadgarov L, Petrone V, Rosentsveig R, Feldman Y, Tenne R, Senatore A. Tribological studies of rhenium doped fullerene-like MoS₂ nanoparticles in boundary, mixed and elasto-hydrodynamic lubrication conditions. *Wear* 2013;297:1103–10.
- [21] Tao X, Jiazheng Z, Kang X. The ball-bearing effect of diamond nanoparticles as an oil additive. *J Phys D: Appl Phys* 1996;29:2932–7.
- [22] Wu YY, Tsui WC, Liu TC. Experimental analysis of tribological properties of lubricating oils with nanoparticle additives. *Wear* 2007;262:819–25.
- [23] Chou C, Lee S. Tribological behavior of nanodiamond-dispersed lubricants on carbon steels and aluminum alloy. *Wear* 2010;269:757–62.
- [24] Elomaa O, Oksanen J, Hakala TJ, Shenderova O, Koskinen J. A comparison of tribological properties of evenly distributed and agglomerated diamond nanoparticles in lubricated high-load steel–steel contact. *Tribol Int* 2014;71:62–8.
- [25] Eswariah V, Sankaranarayanan V, Ramaprabhu S. Graphene-based engine oil nanofluids for tribological applications. *ACS Appl Mater Interfaces* 2011;3:4221–7.
- [26] Liu R, Wei X, Tao D, Zhao Y. Study of preparation and tribological properties of rare earth nanoparticles in lubricating oil. *Tribol Int* 2010;43:1082–6.
- [27] Ghaednia H, Jackson RL. The effect of nanoparticles on the real area of contact, friction, and wear. *ASME J Tribol* 2013;135:041603–10.
- [28] Lee J, Cho S, Hwang Y, Lee C, Kim SH. Enhancement of lubrication properties of nano-oil by controlling the amount of fullerene nanoparticle additives. *Tribol Lett* 2007;28:203–8.
- [29] Jiao D, Zheng S, Wang Y, Guan R, Cao B. The tribology properties of alumina/silica composite nanoparticles as lubricant additives. *Appl Surf Sci* 2011;257:5720–5.
- [30] Kogovsek J, Remškar M, Mrzel A, Kalin M. Influence of surface roughness and running-in on the lubrication of steel surfaces with oil containing MoS₂ nanotubes in all lubrication regimes. *Tribol Int* 2013;61:40–7.
- [31] Zhang B, Xu B, Xu Y, Gao F, Shi P, Wu Y. Cu nanoparticles effect on the tribological properties of hydrosilicate powders as lubricant additive for steel–steel contacts. *Tribol Int* 2011;44:878–86.
- [32] Hu C, Bai M, Lv J, Wang P, Li X. Molecular dynamics simulation on the friction properties of nanofluids confined by idealized surfaces. *Tribol Int* 2014;78:152–9.
- [33] Gao Y, Ruestes CJ, Urbassek HM. Nanoindentation and nanoscratching of iron: Atomistic simulation of dislocation generation and reactions. *Comput Mater Sci* 2014;90:232–40.
- [34] Wu CD, Lin JF, Fang TH. Molecular dynamic simulation and characterization of self-assembled monolayer under sliding friction. *Comput Mater Sci* 2007;39:808–16.
- [35] Capozza R, Fasolino A, Ferrario M, Vanossi A. Lubricated friction on nanopatterned surfaces via molecular dynamics simulations. *Phys Rev B* 2008;77:235432–7.
- [36] Lee WG, Cho KH, Jang H. Molecular dynamics simulation of rolling friction using nanosized spheres. *Tribol Lett* 2008;33:37–43.
- [37] Rigney DA, Fu XY, Hammerberg JE, Holian BL, Falk ML. Examples of structural evolution during sliding and shear of ductile materials. *Scr Mater* 2003;49:977–83.
- [38] Lv J, Bai M, Cui W, Li X. The molecular dynamic simulation on impact and friction characters of nanofluids with many nanoparticles system. *Nanoscale Res Lett* 2011;6:200–8.
- [39] Hu C, Bai M, Lv J, Liu H, Li X. Molecular dynamics investigation of the effect of copper nanoparticle on the solid contact between friction surfaces. *Appl Surf Sci* 2014;321:302–9.
- [40] Shao X, Tian J, Liu W, Xue Q, Ma C. Tribological properties of SiO₂ nanoparticle filled-phthalazine ether sulfone/phthalazine ether ketone (50/50 mol %) copolymer composites. *J Appl Polym Sci* 2002;85:2136–44.
- [41] Peng DX, Kang Y, Hwang RM, Shyr SS, Chang YP. Tribological properties of diamond and SiO₂ nanoparticles added in paraffin. *Tribol Int* 2009;42:911–7.
- [42] Peng DX, Kang Y, Chen CH, Chen SK, Shu F. The tribological behavior of modified diamond nanoparticles in liquid. *Ind Lubr Tribol* 2009;61:213–9.
- [43] Chu HY, Hsu WC, Lin JF. The anti-scuffing performance of diamond nanoparticles as an oil additive. *Wear* 2010;268:960–7.
- [44] Ivanov MG, Pavlyshko SV, Ivanov DM, Petrov I, Shenderova O. Synergistic compositions of colloidal nanodiamond as lubricant-additive. *J Vac Sci Technol B* 2010;28:869–77.
- [45] Peng DX, Chen CH, Kang Y, Chang YP, Chang SY. Size effects of SiO₂ nanoparticles as oil additives on tribology of lubricant. *Ind Lubr Tribol* 2010;62:111–20.
- [46] Mochalin VN, Shenderova O, Ho D, Gogotsi Y. The properties and applications of nanodiamonds. *Nat Nanotechnol* 2012;7:11–23.
- [47] Chou CC, Lee SH. Rheological behavior and tribological performance of a nanodiamond-dispersed lubricant. *J Mater Process Technol* 2008;201:542–7.
- [48] Liu K, Liu X, Wang W, Jiao M. Experimental investigation on particle effect in piston ring-cylinder lubrication. *Chin J Mech Eng* 2006;19:191–4.
- [49] Sia SY, Sarhan AAD. Morphology investigation of worn bearing surfaces using SiO₂ nanolubrication system. *Int J Adv Manuf Technol* 2014;70:1063–71.
- [50] Padgurskas J, Rukuija R, Prosyčėvas I, Kreivaitis R. Tribological properties of lubricant additives of Fe, Cu and Co nanoparticles. *Tribol Int* 2013;60:224–32.
- [51] Viesca JL, Hernández Battez A, González R, Chou R, Cabello JJ. Antiwear properties of carbon-coated copper nanoparticles used as an additive to a polyalphaolefins. *Tribol Int* 2011;44:829–33.
- [52] Hoover WG. Canonical dynamics: Equilibrium phase-space distributions. *Phys Rev A* 1985;31:1695–7.
- [53] Bonny G, Pasianot RC, Castin N, Malerba L. Ternary Fe–Cu–Ni many-body potential to model reactor pressure vessel steels: first validation by simulated thermal annealing. *Philos Magn* 2009;89:3531–46.
- [54] Tersoff J. Modeling solid-state chemistry: interatomic potentials for multi-component systems. *Phys Rev B* 1989;39:5566–8.

- [55] Zhang S, Zhang Y, Huang S, Wang P, Tian H. Molecular dynamics simulations of silica nanotube: structural and vibrational properties under different temperatures. *Chin J Chem Phys* 2010;23:497–503.
- [56] Flirkema E, Bromley ST. A new interatomic potential for nanoscale silica. *Chem Phys Lett* 2003;378:622–9.
- [57] Banerjee S, Naha S, Puri IK. Molecular simulation of the carbon nanotube growth mode during catalytic synthesis. *Appl Phys Lett* 2008;92:233121.
- [58] Xie L, Brault P, Thomann AL, Bauchire JM. AlCoCrCuFeNi high entropy alloy cluster growth and annealing on silicon:a classical molecular dynamics simulation study. *Appl Surf Sci* 2013;285:810–6.
- [59] Berro H, Fillot N, Vergne P. Molecular dynamics simulation of surface energy and ZDDP effects on friction in nano-scale lubricated contacts. *Tribol Int* 2010;43:1811–22.
- [60] Plimpton SJ. Fast parallel algorithms for short-range molecular dynamics. *J Comp Phys* 1995;117:1–19.
- [61] Swope WC, Andersen HC, Berens PH, Wilson KR. A computer simulation method for the calculation of equilibrium constants for the formation of physical clusters of molecules: Application to small water clusters. *J Chem Phys* 1982;76:637–49.
- [62] Hammerberg JE, Germann TC, Holian BL, Ravelo R. Nonequilibrium molecular dynamics simulations of metallic friction at Ta/Al and Cu/Ag interfaces. *Mater Trans A* 2004;35:2741–5.
- [63] Lin EQ, Niu LS, Shi HJ, Duan Z. Molecular dynamics simulation of nano-scale interfacial friction characteristic for different tribopair systems. *Appl Surf Sci* 2012;258:2022–8.
- [64] Kim H, Kim WK, Falk M, Rigney D. MD simulations of microstructure evolution during high-velocity sliding between crystalline materials. *Tribol Lett* 2007;28:299–306.
- [65] Karthikeyan S, Agrawal A, Rigney DA. Molecular dynamics simulations of sliding in an Fe–Cu tribopair system. *Wear* 2009;267:1166–76.